Journal of Molecular Structure 1232 (2021) 129976

Contents lists available at ScienceDirect

Journal of Molecular Structure

journal homepage: www.elsevier.com/locate/molstr

Synthesis, spectral properties, crystal structure and theoretical calculations of a new geminal diamine: 2,2,2-Trichloro-*N*,*N*′-bis(2-nitrophenyl)-ethane-1,1-diamine

Fatma Aydın[a,*], N Burcu Arslan[b]

[a] Department of Chemistry, Faculty of Arts and Sciences, Çanakkale Onsekiz Mart University, 17100 Çanakkale, Turkey
[b] Department of Computer Education and Instructional Technology, Faculty of Education, Giresun University, 28200, Giresun, Turkey

ARTICLE INFO

Article history:
Received 3 July 2020
Revised 15 January 2021
Accepted 16 January 2021
Available online 3 February 2021

Keywords:
Chloral hydrate
Geminal diamine
o-Nitroaniline
X-ray analysis
Global reactivity

ABSTRACT

A new 2,2,2-trichloro-*N*,*N*′-bis(2-nitrophenyl)-ethane-1,1-diamine was synthesized by the reaction of 2-nitroaniline in DCM with the chloral formed by distillation of chloral hydrate over concentrated H_2SO_4. The structure of the title compound was identified by means of FT-IR, ^{1}H NMR, and ^{13}C NMR spectroscopic techniques. The crystal structure of the title compound has also been examined by using X-ray crystallographic techniques and found to be crystallized in the monoclinic crystal system and space group $P2_1/n$ with the unit cell parameters: $a = 7.7075(12)$ Å, $b = 7.7396(10)$ Å, $c = 28.247(4)$ Å, $\beta = 93.602(5)°$, $V = 1681.7(4)$ Å^3, Dx = 1.602 Mg m^{-3}, and $Z = 4$ respectively. The calculated electronic structure properties of the title molecule such as HOMO-LUMO analysis, molecular electrostatic potential (MEP) map, and the Mulliken charge distributions were investigated by using the density functional theory (DFT) method. Theoretically calculated values exhibit the chemically hard, high kinetic stable and less reactive molecule.

© 2021 Elsevier B.V. All rights reserved.

1. Introduction

Chloral, known as 2,2,2-trichloroacetaldehyde or 2,2,2-trichloroethanal, is an organic compound with the formula Cl_3CCHO, which is a colorless oily liquid. Due to the presence of two functional groups such as carbonyl and trichloromethyl and their mutual activating effect, the chloral molecule has been used in a wide variety of syntheses [1]. It is soluble in a wide range of solvents, but it is very unstable in water and reacts with an equivalent of water to form chloral hydrate. Chloral hydrate is a reagent and it is used in industries to prepare organic compounds such as isatin, DDT, *etc*. [2,3]. In medicine, it used for short-term treatment of insomnia and has anticonvulsant and muscle relaxant properties. It was once used as a sedative and hypnotic substance in pharmaceutical drugs [4–7].

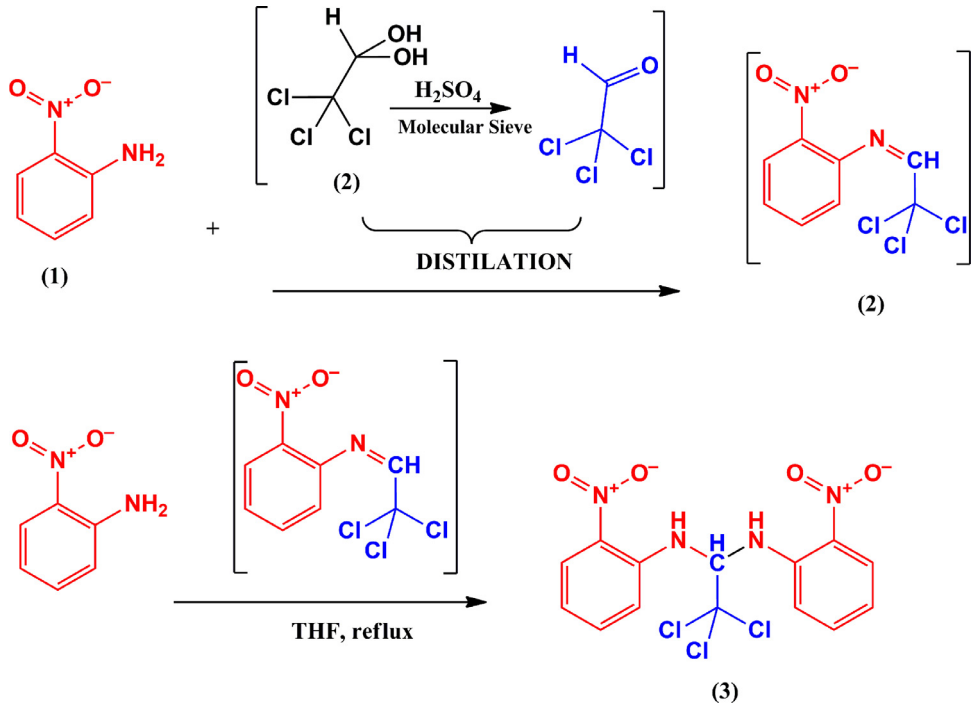
Compounds known as Schiff bases are usually formed by the condensation reaction of a carbonyl compound such as aldehyde or ketone with a primary amine. Schiff bases, firstly reported by Hugo Schiff in 1864, that contain an azomethine group (-HC=*N*-) are also identified as imines (>*C*=NH-) [8]. Schiff bases of aliphatic aldehydes are relatively unstable and readily undergo polymerization, while those of aromatic aldehydes, having a conjugation system, are more stable [9–11] .

A geminal diamine compound contains two amino groups bound to the same carbon atom. It usually acts as a reactive intermediate product. Therefore, studies on the formation of substituted geminal diamine derivatives are limited [12–16].

Herein, a new gem–diamine compound named as 2,2,2-trichloro-*N*,*N*′-bis(2-nitrophenyl)-ethane-1,1-diamine (**3**) was synthesized from a Schiff base obtained by the reaction of chloral with 2-nitroaniline (Scheme 1) and its structure was characterized by elemental analysis, FT-IR, ^{1}H NMR and ^{13}C NMR spectroscopic techniques and structurally single crystal XRD method. Hydrogen bond geometry of the molecule was determined by the X-ray technique. Additionally, optimized geometrical parameters, molecular electrostatic potential (MEP), Mulliken charges, HOMO-LUMO energy gap and the global reactivity from the frontier orbitals of the title molecule have been performed by using the density functional theory (DFT) B3LYP method with the 6–311G(d,p) basis set. The standard thermodynamic functions: heat capacity (Cp), entropy (S^0) and enthalpy (ΔH^0) were calculated to investigate thermodynamical properties of the title compound.

* Corresponding author.
E-mail address: faydin@comu.edu.tr (F. Aydın).

https://doi.org/10.1016/j.molstruc.2021.129976
0022-2860/© 2021 Elsevier B.V. All rights reserved.



Scheme 1. The synthesis of 2,2,2-trichloro-*N,N′*-bis(2-nitrophenyl)-ethane-1,1-diamine.

2. Experimental details

2.1. Materials and measurements

All reagents for synthesis were commercially obtained and were used without further purification. The ^{1}H- and ^{13}C NMR spectra were recorded in deuterated chloroform ($CDCl_3$) at 25 °C on a JEOL NMR spectrometer operating at 400 and 100 MHz. Infrared absorption spectra were obtained by a Perkin Elmer BX II spectrometer and reported in cm^{-1} units. The melting point was measured in an Electro Thermal IA 9100 instrument using a capillary tube. Elemental analysis was conducted on a LECO-932 CHNS analyzer.

*2.2. Synthesis of 2,2,2-trichloro-*N,N′*-bis(2-nitrophenyl)-ethane-1,1-diamine*

The chloral (0.740 g, 5 mmol) obtained by distillation of chloral hydrate using a molecular sieve in the presence of concentrated H_2SO_4 was dissolved in dichloromethane (15 mL) and added to 2-nitroaniline (1.380 g, 10 mmol) in dichloromethane (15 mL). The mixture was heated under reflux for 1 hour. The progress of the reaction was monitored by T.L.C. (1:1, hexane:ethyl acetate). After the completion of the reaction, the brilliant yellow precipitate of the condensation product was filtered and washed with alcohol (2 × 3 mL). The precipitate was dried in a vacuum desiccator and purified by crystallization from THF. Yield 1.195 g (59.1%), mp. 118–120 °C. Elemental analysis for $C_{14}H_{11}Cl_3N_4O_4$: Calculated, (%): C: 41.45, H: 2.73, N: 13.81, Cl: 26.22, O: 15.78; Found, (%): C: 41.58, H: 2.79, N: 13.74, Cl: 26.18, O: 15.71. FT-IR (ATR) ν 3337, 3335, 3175, 3097, 2971, 1609, 1577, 1490, 1443, 1417, 1341, 1299, 1268, 1152, 1038, 1226, 891, 838, 801, 734, 685 cm^{-1}; ^{1}H NMR (400 MHz, $CDCl_3$) δ (ppm) 5.88 (t, *J* = 8.29 Hz, 1H, NH–C **H**–NH), 6.99 (d, 2H, *J* = 8.50 Hz, -N **H**–CH–N **H**-), 6.87 (t, *J* = 7.71 Hz, 2H, C**H**$_{ar}$), 7.51 (t, *J* = 7.79 Hz, 2H, C**H**$_{ar}$), 8.24 (dd, J_{HH} = 8.49 and 1.42 Hz, 2H, C**H**$_{ar}$), 8.79 (d, *J* = 8.21 Hz, 2H, C**H**$_{ar}$); ^{13}C NMR (100 MHz, $CDCl_3$) δ (ppm), 142.13 (s), 136.66 and 136.55 (d, *J* = 0.10.6 Hz), 133.77 (s), 127.50 and 127.38 (d, *J* = 12.03 Hz), 118.55 and 118.42 (d, *J* = 13.57 Hz), 114.22 and 114.06 (d, *J* = 16.38 Hz), 100.98 (s), 74.01 and 73.86 (d, *J* = 15.17 Hz).

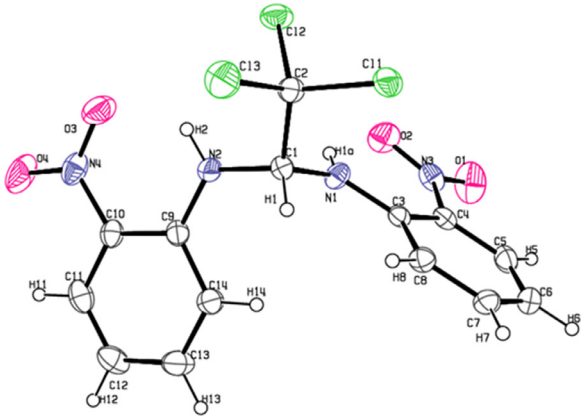


Fig. 1. ORTEP drawing of the asymmetric unit for the 2,2,2-trichloro-N,N′-bis(2-nitrophenyl)ethane-1,1-diamine (3), Ellipsoids are displayed at the 30% probability level.

2.3. Structure determination and refinement

Single crystal suitable for X-ray diffraction studies was obtained by a slow evaporation technique using tetrahydrofuran as a solvent. X-ray data was collected with a Bruker Smart Apex II CCD area detector diffractometer with a graphite-monochromated MoKα radiation source (λ 0.71073 Å) at 293°K. The structure was solved by direct method using SHELXS97 [17] and all of the non-hydrogen atoms were refined anisotropically by full-matrix least-squares on F^2 using SHELXL97 [18]. All H atoms were placed in their calculated positions and included in the refinement using the riding model (Fig. 1). Crystal data and structure refinement parameters for the title compound are listed in Table 1. Diagrams for the molecular structure and crystal packing are shown in Fig 2, Fig.S1a and Fig. S1b. Unit cell packing details, such as geometric parame-

Table 1
Crystal data and structure refinement parameters for the title compound.

Crystal data	
Chemical formula	$C_{14}H_{11}Cl_3N_4O_4$
Mr	405.62
Crystal system, space group	Monoclinic, $P2_1/n$
Temperature (°K)	296
a, b, c (Å)	7.7075 (12), 7.7396 (10), 28.247 (4)
α, β, γ (°)	90, 93.602 (5), 90
V (Å^3)	1681.7 (4)
Z	4
Radiation type	Mo K_α
No. of reflections for cell measurement	9895
θ range (°) for cell measurement	3.0–27
μ (mm^{-1})	0.57
Crystal shape	Block
Crystal size (mm)	0.17 × 0.14 × 0.11
Data collection	
Diffractometer	Bruker APEX-II CCD
Absorption correction	Multi-scan
Tmin, Tmax	0.908, 0.939
No. of measured, independent and observed [$I > 2\sigma$(I)] reflections	65,820, 3324, 2931
Rint	0.057
(sin θ/λ)max (Å^{-1})	0.617
Refinement	
R[F^2 > 2σ(F^2)], wR(F^2), S	0.058, 0.120, 1.22
No. of reflections	3324
No. of parameters	227
H-atom treatment	H-atom parameters constrained
	$w = 1/[\sigma^2(F_o^2) + (0.0075P)^2 + 4.1274P]$ where $P = (F_o^2 + 2F_c^2)/3$
(Δ/σ)max	< 0.001
$\Delta\rho$max, $\Delta\rho$min (e Å^{-3})	0.27, −0.31

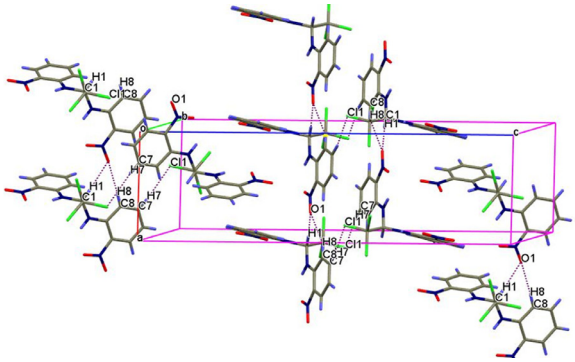


Fig. 2. Molecular packing along the b-axis; A partial view of the crystal packing of title compound, showing the linear arrangement built from C–H.... O weak intermolecular interactions.

Table 2
Geometric parameters and symmetry operations for the intermolecular interactions (A°, °).

D—H•••A	D—H	H•••A	D•••A	D—H•••A
C1—H1•••O1^i	0.98	2.54	3.519 (5)	176
C7—H7•••Cl1^{ii}	0.93	2.91	3.830 (4)	171
C8—H8•••O1^i	0.93	2.45	3.293 (5)	150
N2—H2•••O3	0.86	1.96	2.606(4)	130
N1—H1•••O2	0.86	1.95	2.619(4)	133
N2—H2•••Cl2	0.86	2.62	3.025(3)	110

Symmetry codes:: (i) $x - 1$, y, z; (ii) $-x$, $-y + 1$, $-z + 1$.

ters and symmetry operations for molecular interactions, are listed in Table 2.

2.4. Computational studies

The molecular structure of the title compound was optimized using DFT in the ground state by the B3LYP [19,20] method with the 6–311G(d,p) [21] basis set included in the Gaussian 09 program [22]. The optimized molecular geometry parameters such as bond length and bond angles by the B3LYP/6311G(d,p) level are listed in Table S2.

For the molecular structure of the title compound optimized by the B3LYP /6–311G(d,p) level, frontier molecular orbitals and electrostatic potential were simulated. By using HOMO and LUMO energy values for the title compound, electron affinity (EA), ionization potential (IP), energy gap, chemical potential (μ_0), chemical hardness (η), softness (ζ), electronegativity (χ) and electrophilicity index (ω) were calculated using the equations [23,24], both equations and their values are listed in the Table 5.

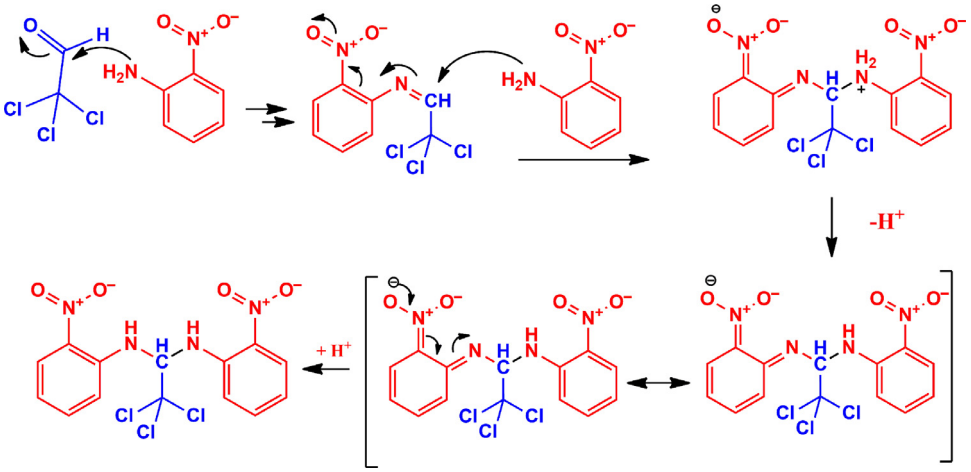
3. Results and discussion

Synthesis of the title compound (**3**) is confirmed from the spectroscopic characterization and the X-ray crystal structure of the compound. The structure of the synthesized compound is defined as a geminal diamine. As shown in Scheme 2, we can summarize that the synthesis occurs with the cascade reactions. An imine has formed in the first step of the reaction. In second step of the reaction, 2-nitroaniline has reacted with obtained imine due to the resonance effect of 2-nitropheyl moiety and the inductive effect of trichloromethyl moiety and a geminal diamine has been obtained.

3.1. Crystallographic results

X-ray investigation shows that the title compound indicates a geminal diamine form. In the title gem–diamine (3), marked structural differences in the molecule of the asymmetric unit are observed (Fig. 1). Central fragments C9/C10/C11/C12/C13/C14 and C3/C4/C5/C6/C7/C8 are almost planar with an r.m.s. deviation of −0.022 and 0.07 Å, with atoms C11 and C4, respectively. Torsion angles between two nitrophenyl amine groups are 77.8° on C9/N2/C1/N1 and −138.8°on N2/C1/N1/C3 atomic chains.

In the packing arrangement of the title compound, different types of weak intermolecular interactions have appeared: C–H...O



Scheme 2. A possible reaction mechanism for the title compound.

and C–H…Cl weak intermolecular interactions as well as N–H…O and N–H…Cl intramolecular interactions. The C1–H1…O1 weak intermolecular interaction gives rise to C(7) chain and the C8–H8…O1 interaction gives rise to C(6) chain, both chains propagate along [100] direction. Since the chains have common atomic pathway, an $\mathbf{R_2^1(7)}$ ring motif also appears (Fig. 2 and Fig S1a). The intramolecular hydrogen bond interaction between the N1–H1…O2 atoms constitutes a six-membered ring S(6) (Fig. S1b). Also, the N2-H2…O3 and N2-H2…Cl2 intramolecular hydrogen bond interactions in the compound create S(6) and S(5) motifs according to graph set notation, respectively [25].

The optimized parameters (bond length, bond angles and torsion angles) of the title compound were obtained using the DFT/B3LYP method with the 6–311G(d,p) basis set. The results are listed in Table S2 and compared with the experimental data for the title compound.

X-ray investigation shows that C1-N1 and C1-N2 bond lengths in the title compound are 1.445 (4) Å and 1.441 (4) Å, respectively. C3-N1 (1.364 (4) Å) and C9-N2 (1.373 (5) Å) bond lengths are slightly shorter than the C1-N1 and C1-N2 bond lengths due to resonance between the nitrogen atoms and 2-nitrophenyl rings. Theoretical values of bond lengths are 1.443 and 1.437 Å, respectively (Table S1). In general, the calculated geometric parameters are in good agreement with those obtained from the experimental results. As can be seen from Table S2, most of the optimized bond distances were found to be slightly longer than the experimental distances. The small differences may be due to fact that the theoretical calculations belong to an isolated molecule without any intermolecular interactions in the gaseous phase and the experimental results belong to molecules in solid state.

3.2. Spectral studies

Infrared spectroscopy has been extensively used for structural determination and provides useful information about the functional groups in the molecular structure under experimental and theoretical studies [26]. Some important experimental (Fig. S2) and calculated (unscaled) vibrational frequencies were collected in Table 3. The vibrational frequencies for the optimized molecular structures are calculated with this method and then scaled by 0.9619.

Generally, ν (N–H) stretching vibrations are observed in the range of 3500–3300 cm^{-1} [27]. In the present study, the N–H symmetric and asymmetric stretching vibrations of the title compound are observed at 3337 and 3332 cm^{-1} in the FT-IR spectrum, respectively. The calculated wavenumbers at 3364 and 3362 cm^{-1} are assigned to N–H stretching vibrations.

Table 3
Comparison of the observed and simulated vibrational spectrum (cm^{-1}) at the B3LYP/6–311G(d,p), (scaling factor for simulated spectrum is 0.9619).

Assignments	Experimental	B3LYP/6 − 311G(d,p)
	FT-IR (cm^{-1})	Scaled freq.
ν_s N—H	3337	3364
ν_{as} N—H	3332	3362
ν C—H (*bz-r*)	3105	3105
ν C—H (*bz-r*)	3059	3079
ν C—H	2971	2975
ν C = C (*bz-r*)	1490	1493
δ C—H	1268	1275
α C—H	1152	1144
ν C(*bz-r*)—N	1417	1453
ν N—CH	1152	1094
γ N—H	1443	1474
ω N—H	685	647
ν_{as} N = O_2	1609	1539
ν_s N = O_2	1341	1329
ν_{as} ClC—CH	838	978
ν_s ClC—CH	734	766

Notes: Vibrational modes: ν, stretching; s, symmetric; as, asymmetric; β in plane bending; α, scissoring; γ, rocking; ω, wagging; δ, twisting; Abbreviations: benzene ring; *bz-r*, benzene ring.

Additionally, the abnormal intensity ratio of ν (N–H) band at 1577 cm^{-1} revealed that intra-molecular hydrogen bond interactions might exist in this compound as observed in the X-ray analysis (Fig. 2).

The C–H stretching vibration for hetero-aromatic structures occurs in the region of 3100 - 3000 cm^{-1}, which is extended to 2800 cm^{-1} in some molecules and is usually overlapped by the stretching of aliphatic CH groups. The C–H stretching vibrations of the title compound are observed at 3105 and 3059 cm^{-1} in the FT-IR spectrum, whereas the calculated wavenumbers at 3105 and 3079 cm^{-1} are assigned to the C–H stretching vibration.

The C–H of the methanetriyl group stretching vibration is generally observed in the range of 3000–2800 cm^{-1}. The band observed at 2971 cm^{-1} in FT-IR spectrum is assigned to a C_1–H_1 symmetrical stretching vibration of the methanetriyl group. The theoretically computed values by the B3LYP/6–311G(d,p) method for the C–H symmetrical stretching vibration is at 2975 cm^{-1}. In the higher wavenumber region of the spectra, differences between

Table 4
Theoretical and experimental ^{1}H and ^{13}C isotopic chemical shifts (with respect to TMS, all values in ppm) for the title compound.

		Calculated chemical shifts(ppm) / B3LYP/6–311G(d,p)		
Atoms	Experimental (ppm) ($CDCl_3$)	Calculated chemical shifts (ppm) (in gas phase)	Calculated chemical shifts (ppm) (in $CDCl_3$)	Calculated chemical shifts (ppm) (in DMSO)
C1	100.98	134.9758	135.1855	135.4189
C2	73.93	149.3995	77.1222	77.1528
C3	142.13	149.3995	149.8510	150.1328
C4	136.60	148.0602	148.6036	148.9331
C5	127.44	141.0406	143.1676	144.2074
C6	118.48	140.9321	142.8978	143.8327
C7	133.77	140.2721	141.148	141.5903
C8	114.14	139.8504	140.7986	141.2711
C9	142.13	133.4607	133.3723	133.2704
C10	136.60	77.1684	116.9662	117.8165
C11	127.44	115.6265	117.9896	118.8517
C12	118.48	116.7680	121.7068	122.2114
C13	133.77	120.5944	121.8781	122.4754
C14	114.14	133.0499	133.0184	132.9270
C1-H1	5.88	5.0415	5.2534	5.3797
N1-H1A	6.99	6.0689	6.2139	6.3021
N2-H2	6.99	6.0682	6.2145	6.3025
C5-H5	8.79	8.3536	8.3474	8.3318
C6-H6	8.24	8.4084	8.4018	8.3863
C7-H7	7.51	9.0424	8.955	8.9178
C8-H18	6.87	6.5830	6.7250	6.7760
C11-H11	8.79	7.1044	7.2985	7.3826
C12-H12	8.24	6.7066	6.8589	6.9143
C13-H13	7.51	7.0247	7.1909	7.2871
C14-H14	6.87	7.447	7.6535	7.7425

experimental and theoretical frequencies are seen due to anharmonicity. By considering Fig. 2 and Table 2, these differences can be due to the weak intermolecular interaction (C1-H1…O1). Additionally, other vibration modes nearly coincide with FT-IR experimentalvalues (Table 3).

The carbon-carbon stretching modes of the phenyl group are expected in the range from 1650 to 1200 cm^{-1}. In this respect, the bands observed at 1490 cm^{-1} are assigned to a $C = C$ stretching vibration, that of the phenyl groups, where they affect to aromatic conjugation. The band at 1493 cm^{-1} is calculated for the $C = C$ stretching.

The mixing of several bands such as C–N, C–C, and N–O stretching vibrations are possible in the same region. The assignment of C–N stretching frequency is a rather difficult task. In the present study, the bands observed at 1417 and 1152 cm^{-1} in FT-IR spectrum are attributed to C_{bz}-N and N–CH stretching vibrations. Their calculated values are at 1453 and 1094 cm^{-1}.

The characteristic asymmetric and symmetric frequencies of nitro compounds are observed at 1540–1614 and 1320–1390 cm^{-1}, respectively [28]. The intramolecular interaction has little effect on the NO_2 asymmetric stretching vibrations. Thus, the bands at 1609 and 1341 cm^{-1} are assigned to the asymmetric and symmetric stretching modes of -NO_2 in the compound. The calculated frequencies for these modes of NO_2 are 1539 and 1329 cm^{-1}, respectively.

The CCl_3 group possesses many normal modes of vibration as in the case of methyl group. However, different halogen atoms have considerably lowered the wavenumber values [29]. It can be classified as the absorption regions of stretching, bending, rocking etc. The asymmetric and symmetric stretching modes of CCl_3 group were calculated at 978 and 893 cm^{-1} and the corresponding experimental peaks were observed as weak bands at 838 and 734 cm^{-1} in FT-IR spectra, respectively.

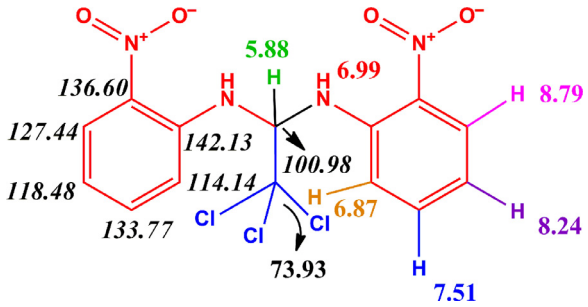
3.3. ^{1}H and ^{13}C NMR chemical shift analyses

The ^{1}H and ^{13}C NMR chemical shift records for 2,2,2-trichloro-*N,N′*-bis(2-nitrophenyl)-ethane-1,1-diamine were experimentally obtained in deuterated chloroform ($CDCl_3$). To investigate NMR chemical shifts of the molecule, the GIAO (Gauge-Independent Atomic Orbital) method was used [20]. ^{1}H and ^{13}C chemical shift values were calculated using the DFT/B3LYP method with the 6–311G(d,p) basis set.

To compute NMR chemical shifts of carbon and hydrogen atoms within the compound, the molecular geometry of the compound was optimized in the gas phase, chloroform, and dimethyl sulfoxide by using IEFPCM solvation model. The computed and measured ^{1}H and ^{13}C NMR chemical shift values were given in Table 4, Fig. S3 and Fig. S4.

The N1-H1A and N2-H2 hydrogen atoms in the compound that are around the neighborliness of electronegative N1 and N2 nitrogen atoms were observed as doublet peaks at δ 6.99 ppm for proton chemical shift of the spectrum, they were calculated at N1-H1A δ 6.07 ppm and N2-H2 δ 6.06 ppm (in gas phase), δ 6.21 and 6.22 ppm and δ 6.30 and 6.30 ppm (in $CDCl_3$ and DMSO–*d6* solvents), respectively in harmony with its experimental value. In addition, C1-H1, for a hydrogen in the methanetriyl group of the compound was observed at δ 5.88 ppm (exp.) as triplet peaks and computed at δ 5.04 ppm (calc. in gas phase) and 5.25 and 5.37 ppm (calc. in $CDCl_3$ and DMSO–d_6 solvents), respectively.

Aromatic ring hydrogens of sp^2 hybridization give resonance signals at the interval of δ 6.5–8.5 ppm [30]. Eleven protons (H5, H6, H7, H8 in phenyl and H11, H12, H13, and H14 in other phenyl) within the aromatic groups of the compound were recorded as signals in the resonance region of δ 6.87–8.79 ppm. The C5-H5 and C11-H11 hydrogen atoms were reported as greater chemical shift signal than other ring hydrogens at 8.79 ppm (exp.) as doublet peak and δ 8.35 ppm (calc. in gas phase) and 8.34 and 8.33 ppm (calc. in $CDCl_3$ and DMSO–d6 solvents) due to the mesomeric effect of amino groups and the powerful electron withdrawing effect of the nitro group, respectively. The other aromatic hydrogens were calculated at the interval of δ 8.40–6.58 ppm (in gas phase), 8.40–6.85 and 8.38–6.91 ppm (in $CDCl_3$ and DMSO–d6 solvents), respectively, according to the DFT/6–311G(d,p) method and they are in a good harmony with the experimental values (Scheme 3).



Scheme 3. ^{1}H and ^{13}C NMR chemical shifts of the title compound.

Table 5
orbital energies, HOMO-LUMO energy gap, ionization potential (I), Electron affinity (A), chemical potential (μ), chemical hardness (η), absolute softness (ζ), absolute electronegativity (χ), chemical potential (μ), and electrophilicity index (ω) of title compound for ground state geometries in the gas phase at the B3LYP/6–311G(d,p) level.

Parameters B3LYP/6–311G(d,p)	(eV)	Kcal/mol
Electronic Energy (a.u.)	−2440,521	
E_{HOMO}	- 6.705	154.61
E_{LUMO}	- 2.698	62.21
Ionization energy, I= -E_{HOMO}	+6.705	154.61
Electron affinity, A= -E_{LUMO}	+2.698	62.21
Energy band gap, [ΔE=E_{HOMO}-E_{LUMO}]	+4.007	92.40
Chemical hardness, η = (I-A) / 2	2.003	46.18
Chemical softness, $\zeta = 1/2\eta$	0.499	11.50
Nucleophilicity, $\varepsilon = 1/\omega$	0.181	4.17
Proton affinity P_I	−4.702	108.42
Chemical potential, μ = - ($I + A$) / 2	−4.007	92.40
Electrophilicity index, $\omega = \mu^2/2\ \eta$	5.518	127.24
Electronegativity, χ = ($I + A$) / 2	4.702	108.42
Dipol moment (Debye)	7.891	

The structure of the compound was confirmed by the presence of eight peaks in the ^{13}C NMR spectrum. In the ^{13}C NMR spectrum, the methanetriyl carbon connected with diamine (C1) has a sp^3 hybrid, but it was located at δ 100.98 ppm because of the geminal diamine and trichloromethyl group. The chemical shift of carbon, C1 was calculated as δ 134.97 ppm (in gas phase), 135.18 and 135.41 ppm (in $CDCl_3$ and DMSO–d_6 solvents), respectively.

The ^{13}C NMR signal of the trichloromethyl group (C2) appeared at δ 73.93 ppm due to effect of the attached electron-withdrawing chloride atoms. Likewise, the calculated chemical shift values for C2 atom, known carbon of trichloromethyl were calculated at δ 149.39 ppm (in gas phase) and 77.12, 77.15 ppm (in $CDCl_3$ and DMSO–d6 solvents), respectively. The carbon atoms in groups are shielded by their own three chlorine atoms and therefore they give a resonance signal in high field [31].

Twelve aromatic carbons were observed in the region of δ 142.13–114.14 ppm as expected. The highest chemical shifts 142.13 ppm were belonging to the amino-bound carbons C3 and C9 as doublets. These carbons were found as δ 134.97 (in gas phase), 135.18 and 135.41 ppm (in $CDCl_3$ and DMSO–d_6 solvents) by theoretical calculations, respectively.

Other aromatic carbons were observed at 136.60, 133.77, 127.44, 118.48 and 114.14 ppm in the spectrum (Scheme 3 and Fig. S4). These carbons were calculated similarly to the experimental values (Table 5). Besides the change in chemical shift values of carbon atoms depending on the substrate concentration and relaxation time, approaches in the theoretical calculation can also be different, so the correlation is not sometimes perfect.

3.4. Frontier Molecular Orbitals (FMOs) analysis and global reactivity

The frontier orbitals, HOMO and LUMO are the most important orbitals in a molecule. These orbitals are the main orbitals taking part in chemical reaction and give information about the reactivity or stability of specific regions of the molecule. The frontier molecular orbitals of the title compound were calculated by using the B3LYP/6–311G(d,p) level of theory.

The distribution of HOMO, HOMO-1 and LUMO, LUMO+1 energies for the compound are shown in Fig. 3.

The ionization potential (I) and electron affinity (A) can be expressed as follows in terms of HOMO and LUMO orbital energy [32],

$$I = -E_{HOMO} \text{ and } A = -E_{LUMO}$$

In addition, theoretical reactivities such as chemical hardness (η), chemical softness (ζ), nucleophilicity (ε), chemical potential (μ), electrophilicity index (ω), electronegativity (χ) and energy band gap (ΔE) were calculated by using the following defined formulas in gas phase, Table 5, [33].

Based on the results in Table 6, the HOMO and LUMO energies for the compound are −6.705 and −2.698 eV, respectively, and the energy gap value of title compound is found to be 4.007 eV. A small gap implies low stability and a large gap implies high stability. A molecule with a large HOMO-LUMO gap is less polarizability and is generally associated with a low chemical reactivity. The chemical hardness (η), softness (σ), and chemical potential (μ) of the title compound were calcalated to be 2.003, 0.499 and −4.702 eV. It should be noted that the electro-negativity provides information about the electron accepting capability of a molecule while nucleophilicity is a measure of Lewis basicity [34]. Calculated electro-negativity (χ) and nucleophilicity (ε) values for this compound are 4.702 and 0.181 eV, respectively. Hence, these values indicate that the title compound is a chemically hard, high kinetic stable, and less reactive molecule.

3.5. Molecular Electrostatic Potential (MEP)

The molecular electrostatic potential (MEP) surface analysis is an important property that can be successfully used to explain the electrostatic interactions. Furthermore, MEP is useful for mapping sites for nucleophilic reactions and electrophilic attacks by showing electron density [35]. To predict the reactive sites of the investigated title compound, MEP was calculated using DFT at the B3LYP/6–311G(d,p) basis set in the gas phase, as shown in Fig. 4. In the color scheme adopted, red indicates an electron-rich region with a partially negative charge and blue an electron-deficient region with partially positive charge, light blue indicates a slightly electron-deficient, yellow a slightly electron-rich region and green a neutral region [36]. Negative regions of the MEP (red color) are related to electrophilic reactivity, while positive regions (blue color) explain the nucleophilic attacks.

In Fig. 4, it appears that the negative region is mainly around the nitro groups (red) [37]. Amine sites, which could be easily attributed to the lone pair electrons on nitrogen atoms are electron-rich and hence could be reactive atomic sites. Positive regions are mainly distributed around some hydrogen atoms (blue). Besides, the most positive region (0.351 a.u.) is the carbon (C2) connected with chloride atoms. The positive region (blue) is over the C1-H group, while the delocalization of electrons from N1 and N2 to the nitrophenyl rings is confirmed by the yellowish color. In addition to these, MEP is related to the electron density on atoms in a molecule and is a very useful descriptor in understanding sites for hydrogen bonding interactions [38]. Regions of positive and negative MEP on the surface of hydrogen bond donors and acceptors are influenced by the formation of intramolecular contacts with the molecules. In the compound, the C6 and C8 carbons are meta position atoms with respect to nitro group, and ortho and para position atoms with respect to amino group. The C6 and C8 carbons became less positive due to the electron withdrawing of the nitro

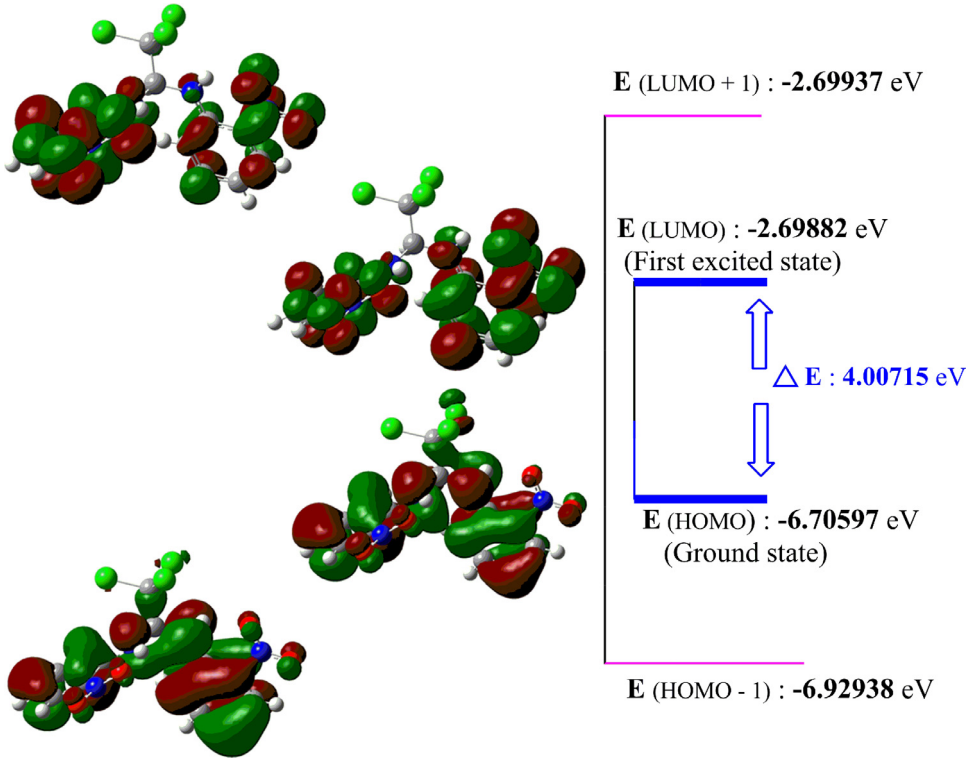


Fig. 3. Highest occupied molecular orbitals (HOMO and HOMO-1) and the lowest unoccupied molecular orbitals (LUMO and LUMO+1) of the title compound.

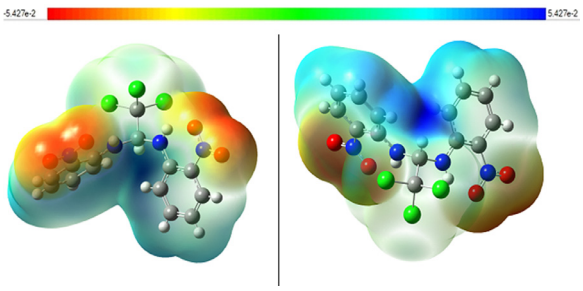


Fig. 4. Molecular electrostatic potential (MEP) mapped on the electron density surface calculated by the DFT/B3LYP method of the title compound.

group and the donation of electrons by the amino group. Therefore, C5-H5 and C7-H7 regions have more positive and they appear in partial blue on the MEP map. Also, the C1-H1 region appears in partial blue due to the inductive effect of the trichloromethyl moiety. This state provides an explanation for inter-molecular interactions of C1-H1…O1 and C7-H7…Cl1 in the crystal structure [39–41].

3.6. Mulliken charge distributions

Dipole moment, molecular polarizability, and bond properties are affected by atomic charge, therefore, the Mulliken atomic charge calculation has an important role in quantum chemistry [42]. The Mulliken charge distributions of the molecule are performed using the DFT/B3LYP calculation method with the 6–311G(d,p) basis set for the studied compounds. Graphical reorientations of Mulliken charge distribution of compound are shown in Fig. 5 and Table S3. As can be seen in Fig. 5, all oxygen atoms have a net negative charge, and all hydrogen atoms have a net positive charge. Naturally, while the nitrogen atoms of the nitro group (N3, N4) have positive charges (0.1655 and 0.1614), the nitrogen atoms

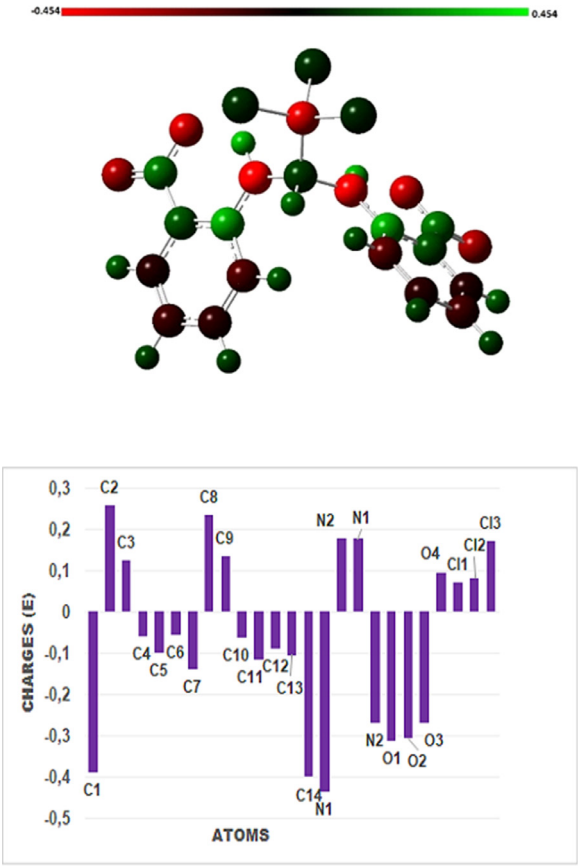


Fig. 5. The Mulliken atomic charge distribution of the title compound in the gas phase.

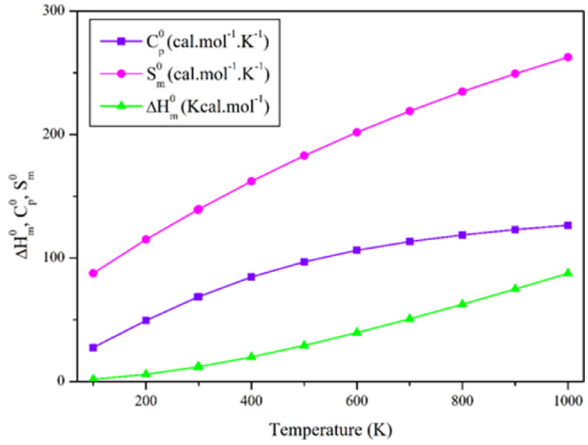


Fig. 6. Calculated thermodynamic properties and temperatures for the title compound.

of the diamine moiety (N1, N2) have negative charges (−0.1421 and −0.1661).

The C2 (−0.3904) carbon atom to which three chloride atoms are attached is the most electronegative among all carbon atoms due to the electronegativity effect of the chloride atoms. On the other hand, the carbon atom C1 (0.2723) attached with two nitrogen atoms is more electropositive than other carbon atoms (C3, C4 and C9, C10) in the compound (0.2343, 0.1197 and 0.2352, 0.1341, respectively) due to the mesomeric effect of the nitrogen atoms.

3.7. Thermodynamic properties

Thermodynamic parameters provide helpful information for understanding the chemical processes. Thermodynamic properties such as heat capacity at constant pressure (Cp), entropy (S), enthalpy (ΔH) for the title compound were also calculated by the DFT method using the B3LYP/6–311G(d,p) basis set and were depicted in Table S3.

As seen from Table S4, the standard thermodynamic functions increase with increase in temperature from 100 to 1000 K, since the molecular vibrational intensities increase with temperature [43]. These observed relations of the thermodynamic functions with temperature were fitted by quadratic formulas and the corresponding fitting factors (R^2) for these thermodynamic properties are 0.99776, 0.99901 and 0.99908, respectively. The temperature dependence correlation graphs are shown in Fig. 6.

$$C^{\circ}_{p.m} = 6.2610 + 0.2417T - 1.2345x10^{-4}T^2 \left(R^2 = 0.99776\right)$$

$$S^{\circ}_{m} = 60.6919 + 0.2872\,T - -8.5930x10^{-5}T^2 \left(R^2 = 0.99901\right)$$

$$\Delta H^0_m = -4.1319 + 0.0409T + 5.1809x10^{-5}T^2 \left(R^2 = 0.99908\right)$$

4. Conclusions

In the present study, a new geminal diamine molecule named as 2,2,2-trichloro-*N,N′*-bis(2-nitrophenyl)-ethane-1,1-diamine, ($C_{14}H_{11}Cl_3N_4O_4$) has been synthesized and structurally characterized by elemental analysis, FT-IR, ^{1}H NMR and ^{13}C NMR spectroscopic techniques. The crystal structure of the compound was determined by the single crystal X-ray diffraction technique. According to the X-ray data, the C–H…O and C–H…Cl weak intermolecular interactions have been observed, besides the formation of N–H …O and N–H…Cl hydrogen bond interactions in the structure. In the solid state, the existence of the crystal field along with the intermolecular interactions have connected the molecules together, which results in differences between the calculated and experimental values for the bond parameters.

By clarifying the structure of the newly synthesized title compound, the Schiff base formed from chloral is considered as an unstable and reactive intermediate. It has been confirmed that the carbonyl group of chloral is highly reactive and susceptible to nucleophile attack. The ^{1}H NMR and ^{13}C NMR spectra clearly confirm the molecular structure. In addition, the HOMO-LUMO analysis, and the regions of the MEP and Mulliken's atomic net charges were calculated by the density functional theory (DFT) method using optimized geometry at the B3LYP/6–311G(d,p) level to investigate the reactive sites of the title compound. As can be seen from the MEP map of the molecule, the negative region is mainly localized over the oxygen atom of the nitro moiety. When the maximum positive region is examined, it is localized on the carbon atom between trichloromethyl and geminal diamine. The chemical reactivity parameters and the thermodynamic properties have been examined for the molecule. The calculated HOMO-LUMO gap energy is 4.007 eV, pointing to a hard molecule as a new geminal diamine compound. Despite the little differences, an acceptable correlation between the computational and experimental results were found.

Declaration of Competing Interest

The authors declare that they have no known competing financial interests or personal relationships that could have appeared to influence the work "Synthesis, spectral properties, crystal structure and theoretical calculations of a new geminal diamine: 2,2,2-Trichloro-*N, N′*-bis(2-nitrophenyl) ethane-1,1-diamine" reported in this paper.

CRediT authorship contribution statement

Fatma Aydın: Methodology, Conceptualization, Data curation, Writing - original draft, Writing - review & editing. **N Burcu Arslan:** Formal analysis, Visualization.

Acknowledgments

This work was supported by the Scientific Research Coordination Unit of Çanakkale Onsekiz Mart University, [Project No: **FYL-2016–672**].

Supplementary materials

Supplementary material associated with this article can be found, in the online version, at doi:10.1016/j.molstruc.2021.129976.

References

[1] F.I. Luknitskii, The Chemistry of Chloral, Chem. Rev. 75 (1975) 259–289, doi:10.1021/cr60295a001.
[2] H.S. Mosher, M.R. Cannon, E.A. Conroy, R.E.V. Strien, D.P. Spalding, Preparation of Technical DDT, Ind. Eng. Chem. 38 (1946) 916–923, doi:10.1021/ie50441a017.
[3] F.A. Gunther, Aspects of the chemistry of DDT, J. Chem. Educ. 22 (1945) 238–242, doi:10.1021/ed022p238.
[4] J. Silverman, W.W. Muir, A review of laboratory animal anesthesia with chloral hydrate and chloralose, Lab. Anim. Sci. 43 (1993) 210–216.
[5] E. Avlonitou, D.G. Balatsouras, E. Margaritis, P. Giannakopoulos, D. Douniadakis, M. Tsakanikos, Use of chloral hydrate as a sedative for auditory brainstem response testing in a pediatric population, Int. J. Pediatr. Otorhinolaryngol. 75 (2011) 760–763, doi:10.1016/j.ijporl.2011.02.010.
[6] J. Cai, Y. Peng, T. Chen, H. Liao, L. Zhang, Q. Chen, Y. He, P. Wu, T. Xie, Q. Pan, Chloral hydrate treatment induced apoptosis of macrophages via fas signaling pathway, Med. Sci. Monit. 22 (2016) 4836–4843, doi:10.12659/MSM.901772.
[7] E. Çeçen, Ö. Uygur, A. Tosun, Severe central nervous and respiratory system depression after sedation with chloral hydrate: a case report, Turk. J. Pediatr. 51 (2009) 497–499.
[8] H. Schiff, Mittheilungen aus dem Universitätslaboratorium in Pisa: eine neue Reihe organischer Basen, Justus Liebigs Ann. Chem. 131 (1864) 118–119, doi:10.1002/jlac.18641310113.

[9] C.T.D. Dahar, Schiff-bases and their applications, J. Sci. Ind. Res. 41 (1982) 501–506 wos:A1982PP93900005.
[10] C. Godoy-Alcántar, A.K. Yatsimirsky, J.M. Lehn, Structure-stability correlations for imine formation in aqueous solution, J. Phys. Org. Chem. 18 (2005) 979–985, doi:10.1002/poc.941.
[11] C.M. Da Silva, D.L. Da Silva, L.V. Modolo, R.B. Alves, M.A. De Resende, C.V.B. Martins, Â.De Fátima, Schiff bases: a short review of their antimicrobial activities, J. Adv. Res. 2 (2011) 1–8, doi:10.1016/j.jare.2010.05.004.
[12] M.G. Shaibakova, I.G. Titova, G.A. Makhmudiyarov, A.G. Ibragimov, U.M. Dzhemilev, Synthesis of 2,3-acetylenic amines by aminomethylation of acetylenes with geminal diamines, Russ. J. Org. Chem. 46 (2010) 43–48, doi:10.1134/S1070428010010021.
[13] K.G. Counts, I. Wong, M.A. Oliveira, Investigating the geminal diamine intermediate of Yersinia pestis arginine decarboxylase with substrate, product, and inhibitors using single wavelength stopped-flow spectroscopy, Biochemistry 46 (2007) 379–386, doi:10.1021/bi061260h.
[14] G. Moad, S.J. Benkovic, On the Mechanism of Decomposition of Geminal Diamines, J. Am. Chem. Soc. 100 (1978) 5495–5499, doi:10.1021/ja00485a038.
[15] P.M. Robitaille, R.D. Scott, J. Wang, D.E. Metzler, Schiff bases and geminal diamines derived from pyridoxal 5'-phosphate and diamines, J. Am. Chem. Soc. 111 (1989) 3034–3040, doi:10.1021/ja00190a043.
[16] M.A. Palafox, J.L. Nez, M. Gil, Theoretical studies on transimination of vitamin B6 analogs, Int. J. Quantum Chem. 89 (2002) 48–56, doi:10.1002/qua.10188.
[17] G.M. Sheldrick, SHELXS-97 - Program for the Solution of Crystal Structures, University of Gottingen, Germany, Univ. Gottingen, Ger, 1997.
[18] G. Sheldrick, SHELXL-97, Program for crystal structure refinement, (2008).
[19] A.D. Becke, Density-functional thermochemistry. I. The effect of the exchange-only gradient correction, J. Chem. Phys. 96 (1992) 2155–2160, doi:10.1063/1.462066.
[20] P. Geerlings, F. De Proft, W. Langenaeker, Conceptual density functional theory, Chem. Rev. 103 (2003) 1793–1873, doi:10.1021/cr990029p.
[21] R. Ditchfield, W.J. Hehre, J.A. Pople, Self-Consistent Molecular-Orbital Methods. IX. An Extended Gaussian-Type Basis for Molecular-Orbital Studies of Organic Molecules, J. Chem. Phys. 54 (1971) 724–728, doi:10.1063/1.1674902.
[22] G.P.M. Frisch, G. Trucks, H. Schlegel, G. Scuseria, M. Robb, J. Cheeseman, G. Scalmani, V. Barone, B. Mennucci, GAUSSIAN09, Revision E. 01, Gaussian Inc., 2009.
[23] I. Fleming, Molecular Orbitals and Organic Chemical Reactions, John Wiley&Sons, London, 1976.
[24] R.G. Parr, L.V. Szentpály, S. Liu, Electrophilicity index, J. Am. Chem. Soc. 121 (1999) 1922–1924, doi:10.1021/ja983494x.
[25] G.P. B.E.R.J. Ellena, 4-Methyl-2-nitroaniline, Acta Cryst C52 (1996) 2074–2076, doi:10.1107/S0108270195016234.
[26] J. Coates, Interpretation of Infrared spectra, a Practical approach, Encyclopedia of Analytical chemistry: applications, theory, and Instrumentation, Wiley, Hoboken, NJ, USA, 2006.
[27] G.C.B. T.C.M.R.M. Silverstein, Spectroscopic Identification of Organic Compounds, 4th Ed John Wiley & Sons, Inc., New York, 1981.
[28] Brian C. Smith, Infrared Spectral Interpretation: A Systematic Approach, CRC Press, 1998 1 st Ed..
[29] M. Dien, Modern Vibrational Spectroscopy and Micro-Spectroscopy: Theory, Instrumentation and Biomedical Applications, John Wiley & Sons, Ltd., 2015, doi:10.1002/9781118824924.
[30] L.M. Jackman, Application of Nuclear Magnetic Resonance Spectroscopy in Organic Chemistry, 2nd ed., Pergamon Press, Ltd. Oxford, 1969.
[31] Kalevi Pihlaja, Erich Kleinpeter, Carbon-13 Chemical Shifts in Structural and Sterochemical Analysis, Wiley-Blackwell, 1994.
[32] C.G. Zhan, J.A. Nichols, D.A. Dixon, Ionization potential, electron affinity, electronegativity, hardness, and electron excitation energy: molecular properties from density functional theory orbital energies, J. Phys. Chem. A. 107 (2003) 4184–4195, doi:10.1021/jp0225774.
[33] B.K. Fukui, The role of the Frontier Orbitals in chemical reactions (Nobel lecture), Angew. Chem. Int. Ed. Engl. 21 (1982) 801–809.
[34] I. Fleming, Molecular Orbitals and Organic Chemical Reactions, John Wiley&Sons, London, 1976.
[35] K. Sen, J.S. Murray, Molecular Electrostatic potentials: Concepts and Applications (Theoretical and Computational Chemistry), 1st Ed, Elsevier, 1996.
[36] R.G. Pearson, Absolute electronegativity and hardness correlated with molecular orbital theory, Proc. Natl. Acad. Sci. 83 (1986) 8440–8441, doi:10.1073/pnas.83.22.8440.
[37] H.A. Khamees, Y.H.E. Mohammed, A. S, F.H. Al-Ostoot, S. Y, S. Alghamdi, S.A. Khanum, M. Madegowda, Effect of o-difluoro and p-methyl substituents on the structure, optical properties and anti-inflammatory activity of phenoxy thiazole acetamide derivatives: theoretical and experimental studies, J. Mol. Struct. 1199 (2020) 127024, doi:10.1016/j.molstruc.2019.127024.
[38] P.W. Kenny, Hydrogen bonding, electrostatic potential, and molecular design, J. Chem. Inf. Model. 49 (2009) 1234–1244, doi:10.1021/ci9000234.
[39] S. Defazio, G. Tamasi, R. Cini, A molecular orbital study of C-H···Cl- and N-H···Cl- hydrogen bonds. Inferences on selected metal complexes and on protein ClC Cl- channels, Comptes Rendus Chim 8 (2005) 1584–1609, doi:10.1016/j.crci.2004.11.042.
[40] F. AydIn, H. Ünver, D. Aykaç, N.O. Iskeleli, Spectroscopic studies and structure of 4-(3-benzoylthioureido)benzoic acid, J. Chem. Crystallogr. 40 (2010) 1082–1086, doi:10.1007/s10870-010-9799-2.
[41] A.F.C. Flores, D.C. Flores, J.R. De Menezes Vicenti, L. Pizzuti, P.T. Campos, (5E)-1-benzyl-5-(3,3,3-trichloro-2-oxopropylidene) pyrrolidin-2-one, Acta Crystallogr. Sect. E Struct. Reports Online. 70 (2014), doi:10.1107/S160053681400751X.
[42] R.S. Mulliken, A new electroaffinity scale: together with data on valence state and on ionization potential and electron affinities, J. Chem. Phys. 2 (1934) 782–793, doi:10.1063/1.1749394.
[43] Y.W. Zi-Kui Liu, Computational Thermodynamics of Materials, 1st Ed, Cambridge University Press, 2016.